

Endothelial Cell Traction Forces on RGD-Derivatized Polyacrylamide Substrata[†]

Cynthia A. Reinhart-King,[‡] Micah Dembo,[§] and Daniel A. Hammer^{*,‡}

Department of Bioengineering, University of Pennsylvania, Philadelphia, Pennsylvania 19104, and Department of Biomedical Engineering, Boston University, Boston, Massachusetts 02215

Received June 28, 2002. In Final Form: October 11, 2002

Receptor-mediated adhesion involves both mechanical and chemical signals occurring at the cell–substrate interface. Using a relatively new technique called traction force microscopy, the magnitude, direction, and spatial location of mechanical forces exerted by endothelial cells on a RGD-peptide-derivatized hydrogel substrate were measured. We constructed a surface with a controlled density of cell adhesion nonapeptide containing RGD, which can ligate endothelial cell integrin receptors and induce cell spreading. Increasing the concentration of the RGD peptide increases cell spreading on an otherwise nonadhesive surface of polyacrylamide, and cell area is a monotonically increasing function of peptide concentration. Correlating the force exerted by the cell to the cell area reveals that force is a linear, increasing function of cell area, with a mean increase in cell force of 10^4 dyn/cm² cell area. Additionally, we have found that tractions exerted by endothelial cells are concentrated at the ends of pseudopodia and are almost negligible under the nucleus. These results indicate that endothelial cells may have an internal structure that contacts and pulls on the substrate at concentrated locations within the tips of cell extensions and that the strength in adhesion increases with cell spreading.

Introduction

Endothelial cell adhesion and migration is a crucial step in many physiological and pathological processes, including angiogenesis, tumorigenesis, and wound healing.¹ In turn, migration is guided and controlled by gradients in the concentration of soluble factors and hormones⁴ and by adhesive interactions of the cell with binding sites on the extracellular matrix (ECM).² Cell migration can also be controlled and guided by external mechanical stimuli, such as fluid shear.³

During migration, forces exerted at these cell–substrate adhesive contacts are in part responsible for holding the cell in place and at the same time are used to propel the cell forward.⁵ Cell migration can thus be described as an asymmetrical, polar distribution of forces across the cell–surface contact area.⁶ A cell extends lamellipodia at the leading edge, forming an anchor between itself and the surface. A “tug-of-war” between the contacts at the front and those further back results in release of the tail of the cell, allowing it to ratchet forward. Thus, migration is in part a result of adhesive imbalance between the front and rear adhesive contacts, modulated by intracellular contractility.

Previously, cell motility has been studied using assays such as the Boyden chamber assay⁷ or the under-agarose

assay,⁸ which quantify migration in terms of statistical measures including cell population density and the random motility coefficient. While these values provide information on the overall movements of a cell population, they say very little about the mechanics of individual cell motility. Similarly, single-cell measurements have been done which determine values such as cell speed and persistence length.^{6,9,10} Each of these measurements provides phenomenological data concerning the migration of cells under various conditions, but they are disconnected from the actual mechanical mechanism and forces that cause such movements. Hopefully, therefore, if measures of motility can be correlated with detailed information on the forces exerted by and on a cell, then it will be possible to achieve a deeper understanding of migration itself and also of the signal transduction pathways that control it.

To ultimately better characterize migration, the role of adhesion on force generation within single cells must be more thoroughly characterized. During cell spreading, adhesive contacts are created and distributed over the cell at the cell–substrate interface.⁷ These adhesive contacts serve as points of cytoskeletal support and contraction,²³ and their formation and arrangement control a variety of cell processes, including cell migration. Previously, it has been shown that migration speed increases with ligand density to some maximum point at which speed then begins to decrease.²² At low ligand densities, the cell is unable to establish a number of contacts sufficient to propel itself across a surface. At high ligand densities, the adhesions are too numerous to allow the release of the cell from the substrate necessary for migration. By better characterizing the role of adhesions and adhesive contacts on force generation, we hope to ultimately better understand the adhesive control of migration.

* To whom correspondence should be addressed. Mailing address: Department of Bioengineering, University of Pennsylvania, 3320 Smith Walk, 120 Hayden Hall, Philadelphia, PA 19104. E-mail: hammer@seas.upenn.edu.

[†] Part of the *Langmuir* special issue entitled The Biomolecular Interface.

[‡] University of Pennsylvania.

[§] Boston University.

(1) Ingber, D. E. *Chest* **1991**, *99* (3 Suppl), 34S–40S.

(2) Ingber, D. E. *Cell* **1993**, *75* (7), 1249–52.

(3) Davies, P. F.; Robotewskyj, A.; Griem, M. L. *J. Clin. Invest.* **1994**, *93* (5), 2031–8.

(4) Yancopoulos, G. D.; Klagsbrun, M.; Folkman, J. *Cell* **1998**, *93*(5), 661–4.

(5) Lauffenburger, D. A.; Horwitz, A. F. *Cell* **1996**, *84* (3), 359–69.

(6) Maheshwari, G.; Lauffenburger, D. A. *Microsc. Res. Tech.* **1998**, *43* (5), 358–68.

(7) Boyden, S. B. *J. Exp. Med.* **1962**, *115*, 453–66.

(8) Rothman, C.; Lauffenburger, D. A. *Ann. Biomed. Eng.* **1983**, *11* (5), 451–77.

(9) Kouvroukoglou, S.; et al. *Biomaterials* **2000**, *21* (17), 1725–33.

(10) Dunn, G. A. *Agents Actions Suppl.* **1983**, *22*, 14–33.

The study of stresses exerted at the cell–substratum interface has, for the most part, been based on measuring deformations in an elastic substratum. This method was first proposed by Harris et al.¹¹ using silicon rubber films. Cell adhesion and contraction caused the film to buckle, and the size and location of the wrinkles were used to make inferences about the forces exerted by the cell. Measurements of this sort proved to be complicated, if not impossible, because wrinkles are intrinsically nonlinear, chaotic nature objects and there is no clear theory relating force and wrinkle size. The wrinkling substratum method was therefore modified by Dembo and Wang,¹² who used polyacrylamide embedded with fluorescent markers. The motions of the embedded beads reflect the deformations of the substrate caused by cellular traction. Because the polyacrylamide deforms linearly, the stresses that cause the bead motions can be reliably deduced with high spatial and temporal resolution. Thus far, the method originated by Dembo and Wang, called traction force microscopy, has been primarily used to study fibroblast migration. Traction force microscopy has led to the development of the frontal towing mechanism of cell migration,¹³ comparisons of fibroblast preference for migration on stiff substrates versus more compliant surfaces,¹⁴ and insight into the role of nascent and mature focal adhesions in the generation of cellular traction forces.¹⁵

The present study relates cell morphology, area, and traction to the substrate surface chemistry in the case of bovine aortic endothelial cells (BAECs). Studies of endothelial cells are ultimately motivated by the need to better understand the adhesion and migration that occur in early angiogenesis. The differential adhesion behavior exhibited by cells may control the ability of cells to find each other on a surface, leading to morphological changes and early blood vessel formation. In these experiments, endothelial cells are plated on polyacrylamide substrates derivatized with varying densities of a nonapeptide containing the arginine-glycine-aspartic acid-serine (RGDS) sequence. The technique developed by Dembo and Wang¹² is then applied in combination with standard measurements of area and morphology to better elucidate the mechanism of cell adhesion in endothelial cells.

Materials and Methods

Cell Culture. BAECs are maintained at 37 °C and 5% CO₂ in Dulbecco's modified Eagle's medium (Bio-Whittaker, Walkersville, MD) supplemented with 10% fetal calf serum, 0.5% penicillin–streptomycin, and 1% 200 mM L-glutamine (Gibco-BRL, Gaithersburg, MD). The cell medium is changed every other day, and approximately every 7 days the cells are replated to 7.5 × 10⁵ cells per 75 mm² flask using trypsin–EDTA (0.05% trypsin and 0.53 mM EDTA-4Na, GibcoBRL).

Activation of Coverslips. Coverslips (no. 1, 45 × 50 mm, Fisher Scientific, Pittsburgh, PA) are chemically activated in preparation for covalent attachment of polyacrylamide sheets using the method adapted from the protocol described by Wang and Pelham.¹⁶ The coverslips are passed through the flame of a Bunsen burner and smeared with a thin layer of 0.1 N NaOH. After the coverslips air-dry, a layer of 3-aminopropyltrimethoxysilane (200 μL, Sigma-Aldrich Chemical Co., St. Louis, MO) is smeared across the coverslip and incubated for 5 min at room temperature. The coverslips are bathed in distilled water for 5

min, 3 times, followed by a 30 min incubation in 0.5% glutaraldehyde (70% aqueous stock solution, Sigma-Aldrich Chemical Co., St. Louis, MO) in phosphate-buffered saline (Invitrogen, Carlsbad, CA) at room temperature. The coverslips are rinsed with distilled water for 10 min, 3 times. The coverslips air-dry horizontally, overnight in a fume hood.

Synthesis of the Bifunctional Linker. The *N*-succinimidyl ester of acrylamido-hexanoic acid (N-6) was synthesized in our laboratory by Swift et al.¹⁷ using the method described by Pless et al.¹⁸ The N-6 covalently links to the gel and has an *N*-succinimidyl ester that is displaced by a primary amine to link the amine-containing ligand to the polyacrylamide substrates.

Gel Synthesis. Gels are prepared using acrylamide (40% w/v solution), *N,N*-methylene-bis-acrylamide (BIS, 2% w/v solution), *N*-tetramethylethylenediamine (TEMED), and ammonium persulfate from Bio-Rad Laboratories (Hercules, CA). The gels contain 5% acrylamide, 0.1% BIS, 54 mM Hepes, 20 μmol/mL of N-6 dissolved in ethanol, 2/25 volume of carboxylate-modified fluorescent latex beads (1.0 μm Fluospheres, Molecular Probes, Eugene, OR), and 1/2000 volume of TEMED. The pH of the monomer solution is adjusted to 6.0 with 1.2 N HCl, the solution is degassed, and a 1/200 volume of 10% ammonium persulfate is added. A 25 μL quantity of the solution is dispensed onto the activated coverslips, and the drop is flattened using a circular coverslip (no. 1, 22 mm diameter, Fisher Scientific, Pittsburgh, PA). The entire assembly is turned upside down and incubated at room temperature for 60 min, allowing polymerization to occur. The circular coverslip is removed, and the gel is rinsed in ice-cold deionized (DI) water for 10 min.

Covalent Attachment of the Ligand to the Gel Substrate. In these experiments, either an RGD-containing nonapeptide (peptide synthesis was provided by the Protein Chemistry Laboratory of the Medical School of the University of Pennsylvania supported by core grants of the Diabetes and Cancer Centers (DK 19525 and CA 16520)) (with a sequence of NH₂–Tyr-Ala-Val-Thr-Gly-Arg-Gly-Asp-Ser–OH) or an RGE-containing nonapeptide (with a sequence of NH₂–Tyr-Ala-Val-Thr-Gly-Arg-Gly-Glu-Ser–OH) is covalently linked to the polyacrylamide gels. The gels are removed from the DI water, coated with 0.5 mL of peptide dissolved to the desired concentration in 50 mM Hepes (pH 8.0), and incubated at 4 °C for 2 h. The gel is then rinsed with DI water, covered with 0.5 mL of a 1/100 volume solution of ethanolamine in 50 mM Hepes (pH 8.0), and incubated at room temperature for 30 min. The gels are rinsed with ice-cold DI water and stored at 4 °C in DI water.

Quantification of Ligand Density within the Gel Using Base Hydrolysis. The density of RGD peptide on the surface of the gel is measured using a highly basic solution to hydrolyze the amide linkage between the peptide and the acrylamide surface. The concentration of peptide released into solution is determined by comparing its absorbance at 280 nm to that of standard solutions. Standard solutions are made by incubating known concentrations of peptide in 5 N NaOH overnight. The solution is then read at 280 nm and plotted to produce a standard curve. The sample gels are made as described above and then incubated overnight in 1 mL of 5 N NaOH. The solution is then read at 280 nm, and the absorbance is compared to the standard curve to calculate the concentration of peptide in the solution.

Culture Chamber Assembly. For traction studies, the coverslips containing the sheets of polyacrylamide gel are sealed to the bottom of a culture chamber (made from a block of lexicon with a hole drilled through the center) using a thin line of Dow-Corning vacuum grease (Fisher Scientific, Pittsburgh, PA). The culture chambers are filled with 3 mL of cell culture medium and sterilized with UV light for 15 min. The chambers are placed at 37 °C and 5% CO₂ for 15 min, the medium is aspirated off, and 1 × 10⁴ cells in 3 mL of medium are added to each chamber. The chambers containing cells incubate at 37 °C and 5% CO₂, and measurements are taken 24 h after the cells are plated.

Characterization of the Gel Substrate. The Young's modulus of the polyacrylamide, which is required for the traction calculations, is calculated by measuring the indentation in the

(11) Harris, A. K.; Wild, P.; Stopak, D. *Science* **1980**, *208* (4440), 177–9.

(12) Dembo, M.; Wang, Y. L. *Biophys. J.* **1999**, *76* (4), 2307–16.

(13) Munevar, S.; Wang, Y. L.; Dembo, M. *Mol. Biol. Cell* **2001**, *12* (12), 3947–54.

(14) Lo, C. M.; et al. *Biophys. J.* **2000**, *79* (1), 144–52.

(15) Benigno, K. A.; et al. *J. Cell Biol.* **2001**, *153* (4), 881–8.

(16) Wang, Y. L.; Pelham, R. J., Jr. *Methods Enzymol.* **1998**, *298*, 489–96.

(17) Swift, D. G.; Posner, R. G.; Hammer, D. A. *Biophys. J.* **1998**, *75* (5), 2597–611.

(18) Pless, D. D.; et al. *J. Biol. Chem.* **1983**, *258* (4), 2340–9.

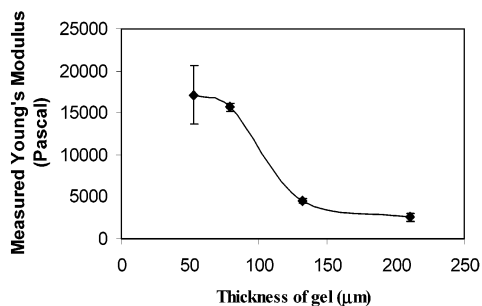


Figure 1. Graph of the Young's modulus versus the thickness of the gel used. Values are calculated from using the steel ball method described in Materials and Methods.

gel due to the weight of a small steel ball (0.025 in. diameter, Hoover Precision Products, East Granby, CT). The ball is placed on the gel embedded with fluorescent beads. The indentation is measured by focusing the microscope to follow the fluorescent beads beneath the gel as they return to their original position when the steel ball is removed. The Young's modulus is calculated given the equation in Munevar et al.,¹⁹ $Y = 3(1 - \nu^2)f^2/4d(B^{3/2}r^{1/2})$, where ν is the Poisson's ratio, f is the buoyancy-corrected weight of the steel ball, d is the depth of the indentation created by the ball, and r is the radius of the ball. The Poisson's ratio is 0.3, as was determined by Li et al.²⁰

To confirm that the Young's modulus measurement was calculated accurately, we made gels of various thicknesses. The modulus of each gel was determined using the steel ball method (Figure 1). The calculations revealed that thinner gels have an apparent higher modulus than thicker gels. This difference is presumably due to the presence of the glass surface beneath the gels. With too thin a gel, the deformation created by the ball is smaller because the gel is too thin to fully deform within its thickness before being affected by the glass. The Young's modulus determined using a thicker gel is more accurate because the depth of the indentation is unaffected by the presence of the glass and the calculated modulus reflects the properties of only the polyacrylamide gel, rather than the gel and the glass. The Young's modulus of gels containing 5% acrylamide and 0.1% BIS-acrylamide was measured to be 2500 Pa using the method described here (see Figure 1).

Microscopy and Analysis. Images of the BAECs on the polyacrylamide surface are gathered using a Nikon Inverted Eclipse TE300 microscope with a Nikon 40 \times , numerical aperture 0.75, phase objective, and pictures are taken using a Photometric Cool Snap HQ camera (Roper Scientific, Trenton, NJ). Phase contrast images of the cell and the corresponding images of the embedded fluorescent beads are taken simultaneously. At the end of the experiment, the cell is released from the polyacrylamide using trypsin-EDTA. Once the cell has completely released, a final fluorescent picture of the relaxed substrate is taken.

Traction forces are determined based on deformations in the polyacrylamide substrate relative to the relaxed substrate. Using custom-written software, the bead displacements within the gel are measured, the cell and nucleus outlines are drawn, and a mesh that fits exactly within the outline of the cell is created. Using the bead displacements and the material properties of the gel, the most likely surface traction vectors are calculated using the technique described by Dembo and Wang.¹²

Results

Control of Cell Area through Peptide Density.

Because polyacrylamide is typically inert to cell adhesion, the surface of the gel had to be modified to support adhesion and growth. In this study, this was accomplished using a chemical linker (N-6). One end of the linker forms a covalent bond with the gel, while the other end is free to be displaced by a primary amine. After polymerization, gels were incubated with solutions of varying concentra-

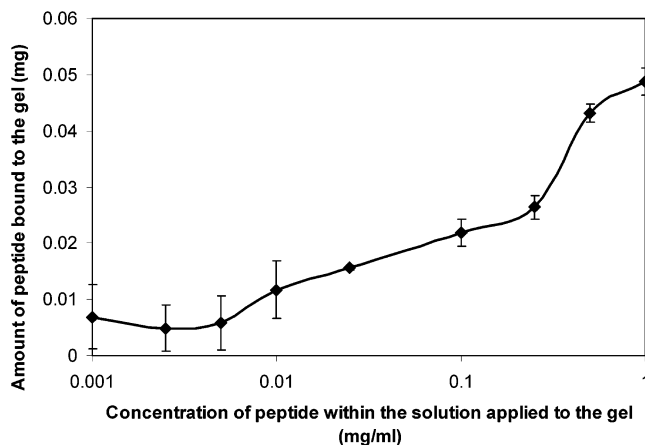


Figure 2. Using a high concentration of basic solution, the amide linkage between the peptide and the gel is hydrolyzed and the peptide is released into solution. The concentration of peptide in solution is measured using absorbance readings at 280 nm and a standard curve. The results are graphed relative to the concentration of peptide in solution in which the gel is reacted.

tions of nonapeptides, ranging from 0.001 to 1.0 mg/mL, which link to the activated N-6 via its N-terminus.

The density of peptide on the surface of the gel is determined using a base hydrolysis assay, which involves liberating the peptide from the gel using a highly basic solution and then measuring the concentration of liberated peptide released into solution. As seen in Figure 2, the concentration of peptide in the gel increases with the concentration of peptide in the original solution in which the gel containing active N-6 is incubated. Moreover, we can approximate the density of peptide on the surface of the gel by converting the overall concentration of the peptide within a volume of gel to a surface density of ligand by assuming a 1 nm penetration depth into the gel in which a cell can bind the peptide. Using these values, the density of ligand on the surface of the gel ranges from approximately 150 to 1500 molecules per square micron.

As a control, to demonstrate the importance of the RGD-containing peptide, a nonapeptide containing arginine-glycine-aspartic acid (RGE) was conjugated to the polyacrylamide substrate sequence, in place of the usual RGD sequence. As seen in Figure 3, BAECs plated on a RGE surface remained in a rounded state. The cells could be easily displaced by light shaking. We conclude specific cell adhesion on our polyacrylamide surfaces is completely dependent on the RGD subsequence within the peptide.

A qualitative comparison of cell spreading on polyacrylamide gels of different peptide densities reveals that the average cell area increases strongly with increasing peptide concentration (see Figures 3 and 4). At the low concentration of 0.001 mg/mL, most cells are attached but only slightly spread on the substrate, whereas at the highest concentration (1.0 mg/mL), the average cell area increases by 3-fold. The increase is more or less monotonic over the entire range, and there is no indication that a plateau or maximum degree of spreading has been reached at the higher RGD densities. As seen in Figure 3, alterations in peptide concentration also lead to changes in cell morphology. Thus, at the lower peptide concentrations, the circumference of the contact area is smooth, whereas at higher concentrations, cells develop more pseudopodia and present a jagged or stellate contour. It should be emphasized that these results refer only to the area and shape of an "average" cell and that under all conditions we observe heterogeneity in cell phenotype.

(19) Munevar, S.; Wang, Y.; Dembo, M. *Biophys. J.* **2001**, *80* (4), 1744-57.

(20) Li, Y.; Hu, Z.; Li, C. *J. Appl. Polym. Sci.* **1993**, *50*, 1107-11.

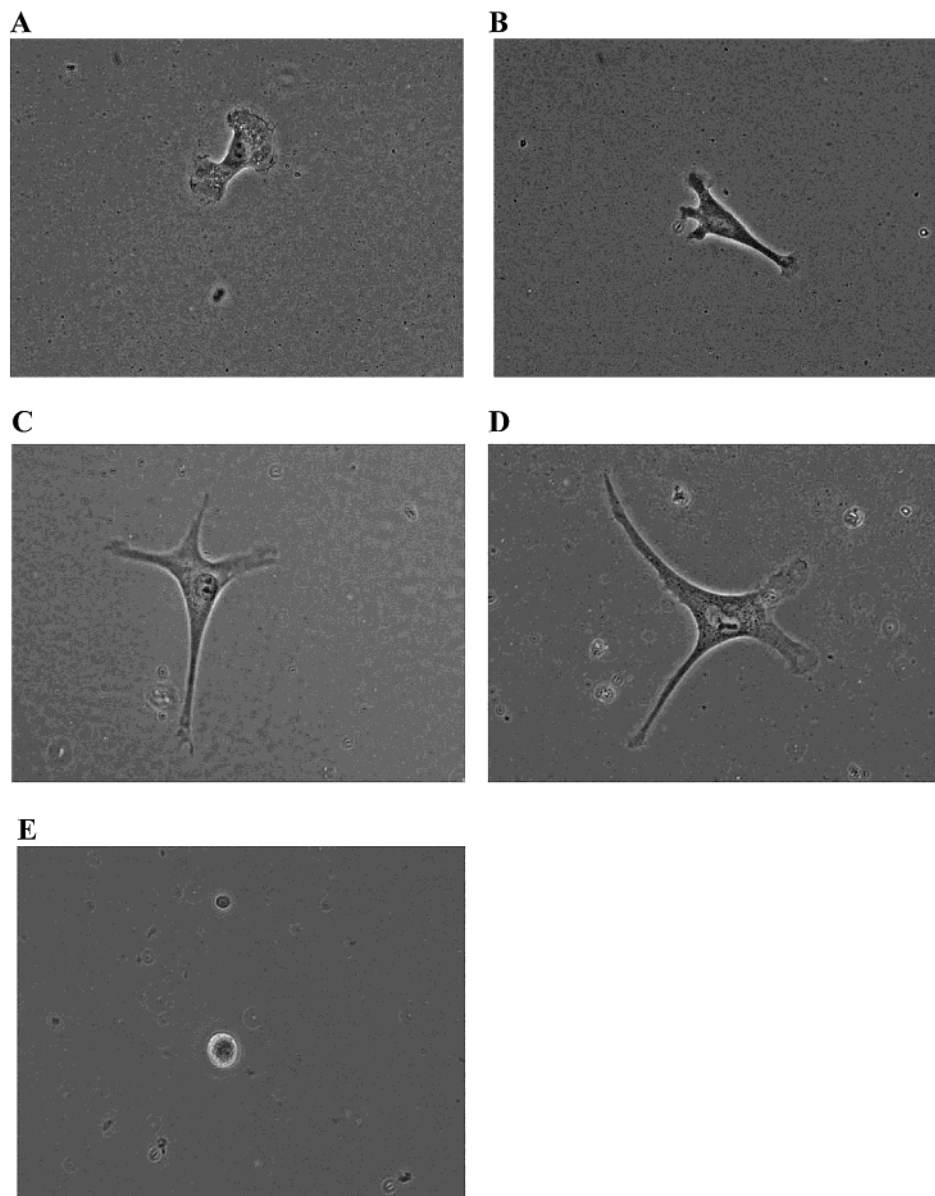


Figure 3. Phase contrast images taken of BAEC cells on RGD-peptide-derivatized polyacrylamide substrates taken at 40 \times magnification. (A) Peptide concentration is 0.001 mg/mL. (B) Peptide concentration is 0.01 mg/mL. (C) Peptide concentration is 0.1 mg/mL. (D) Peptide concentration is 1.0 mg/mL. (E) Phase contrast image of a BAEC cell on an RGE-peptide-derivatized polyacrylamide substrate at 40 \times magnification. Peptide concentration is 1.0 mg/mL.

Thus even at low RGD densities it is possible to find the occasional cell that is well spread with pseudopodia and even at high density it is possible to find a few round cells.

Tractions are Most Pronounced underneath Pseudopodia. The tractions exerted by various cells were calculated using the method of Dembo and Wang based on substrate deformations. The location of regions of high and low traction is best visualized by contour plots of the traction magnitude (see Figure 5). The results indicate that tractions exerted by BAECs become strongest near the ends of the pseudopodia and that they are smallest directly surrounding the nucleus. In well-spread cells with large extensions, the ratio of maximum and minimum traction is between 2 and 3 orders of magnitude. Rounded cells with smaller area show less of a gradient in traction. We conclude that the forces associated with maximal adhesion and spreading appear to be localized at the tips of the pseudopodia.

The angular orientation of the traction stress exerted by a cell on the substrate is best revealed by vector plots

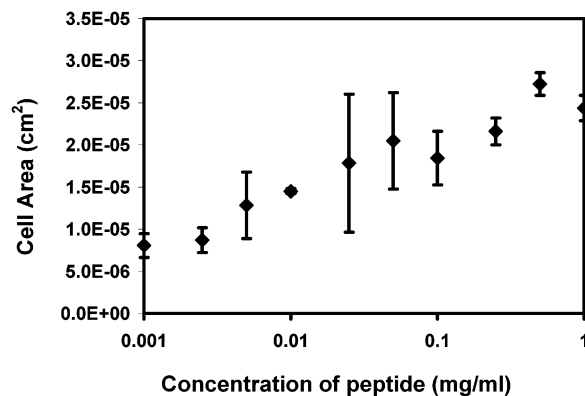


Figure 4. Cells were plated on polyacrylamide derivatized with an RGD-containing peptide. The graph shows the relationship between the RGD-peptide concentration and spread cell area. $n = 3$.

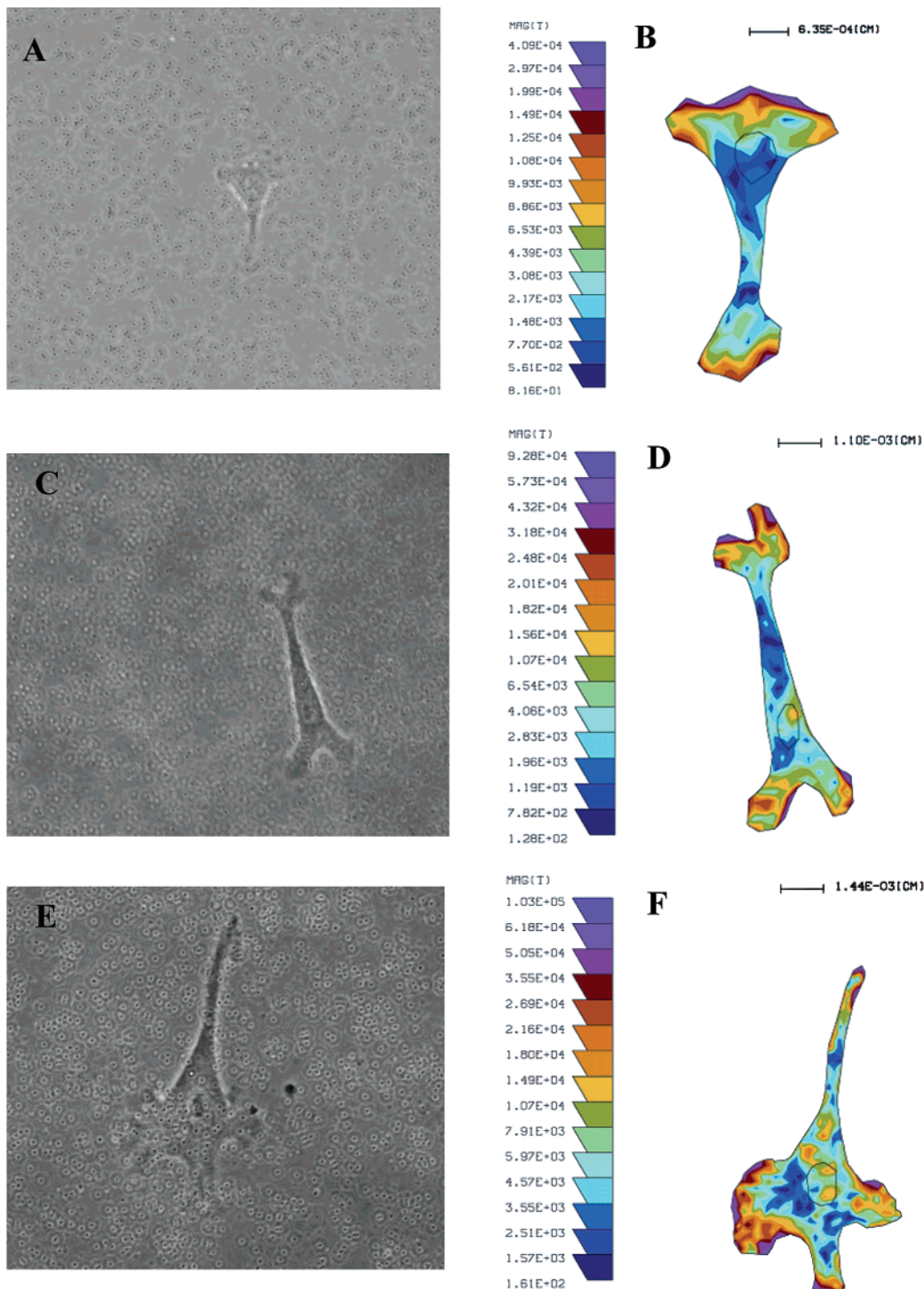


Figure 5. Traction forces of cells plated in polyacrylamide derivatized with an RGD-containing peptide were determined using traction force microscopy. (A,C,E) Phase images of BAECs taken at 40 \times magnification on (A) 0.001 mg/mL of RGD peptide, (C) 0.01 mg/mL of RGD peptide, and (E) 0.25 mg/mL of RGE peptide. (B,D,F). Color contour plot of the magnitudes of the traction stress exerted by the corresponding cells in panels A, C, and E.

of the tractions (see Figure 6). Such plots demonstrate that all cells tend to pull the substrate inward from the outer boundary toward the nucleus. The overall pattern indicates that the cytoskeleton between attachment points at opposite ends of the cell is in a state of perpetual contractile tension. The strength of this contraction varies with degree of spreading, but the basic pattern is independent of the degree of cell spreading.

Force Exerted by a Cell Increases with Area. At higher peptide concentrations, where the cell area is greater, we find that the force produced by BAECs is also

significantly larger. This raises three possibilities: (1) The increase in peptide concentration drives the increase in force, which then drives the increase in cell area. (2) The increase in peptide drives the increase in area which then causes the increase in force. (3) The increase in peptide density causes the increase in area and force via independent pathways.

The third hypothesis is easily checked since it predicts that for a fixed peptide density the cell-to-cell fluctuations of force and area should be independent random variables. Therefore, we collected all observations of force and area

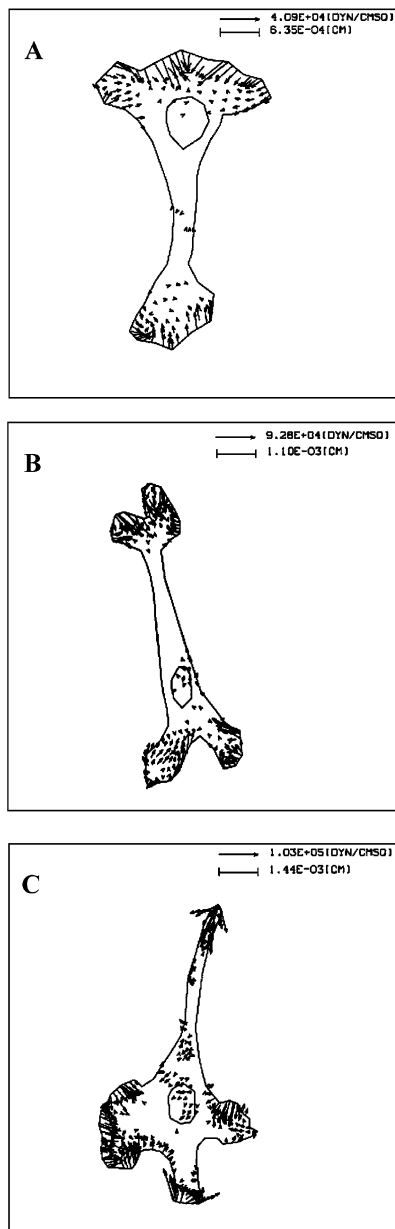


Figure 6. Traction stress renderings of the stresses exerted by the cells in Figure 5 represented by vectors within the cell boundary: (A) corresponds with cell A of Figure 5, (B) corresponds with cell C of Figure 5, and (C) corresponds with cell E of Figure 5.

for all cells observed on substrates having RGD densities between 0.2 and 0.5 mg/mL. This is a very limited range over which there is no significant change in the statistical average of cell area or force. Despite this, there is still plenty of cell-to-cell variation in this population. Nevertheless, plotting force versus area reveals a very strong linear correlation (see Figure 7). The slope of the line in Figure 7 indicates that a typical cell of the sample needs to exert a force of 10^4 dyn to achieve a 1 cm^2 increase in its area. In any event, it is clear from Figure 7 that the force and area are not independent random variables; thus, hypothesis 3 is false and force and area are directly correlated.

The areas and forces of the cells in the population sampled to generate Figure 7 have a limited range since the peptide density was so restricted. Therefore, it is of interest to extend the analysis to the full population of all cells in the current study (Figure 8). This includes cells

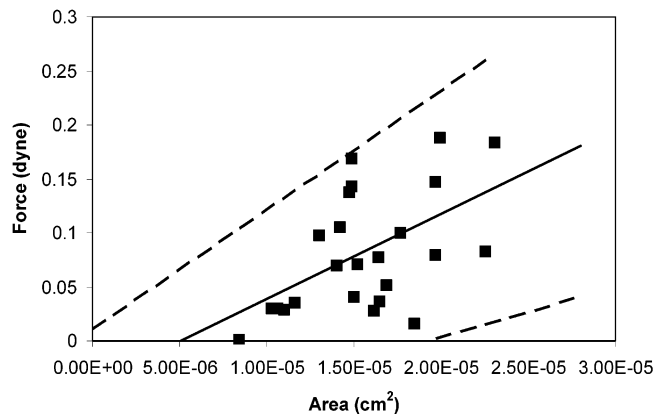


Figure 7. Graph of force exerted by a cell versus the spread cell area for cells on 0.2–0.5 mg/mL of RGD peptide. The solid line represents the linear best fit with an R^2 value equal to 0.29 and a slope of 7878 dyn/cm². The dashed lines represent the regression line $\pm 2\sigma$.

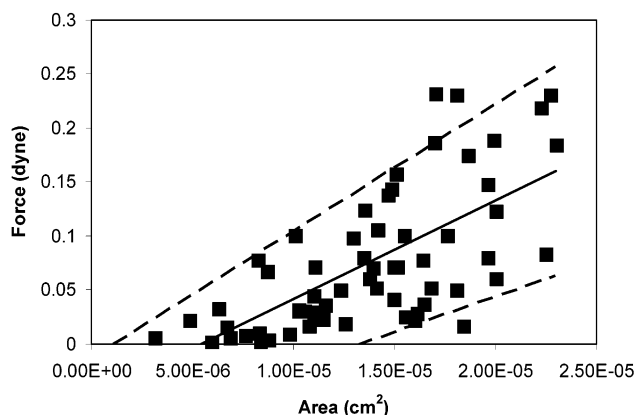


Figure 8. Graph of the relationship between cell area and overall force exerted by the cell. The solid line represents the linear best fit with an R^2 value equal to 0.45 and a slope of 9146 dyn/cm². The dashed line represents the regression line $\pm 2\sigma$.

from all different peptide densities and includes everything from cells that have only minimally attached to the surface of the gel to cells that have completely spread over the gel. Within this range of endothelial spreading, the force between the cell and substrate varies over 18-fold. Nevertheless, plotting force versus area for the larger heterogeneous population (see Figure 8) reveals exactly the same linear correlation of force and area as was observed in the data for a limited peptide range. The slope and intercepts of the lines in Figures 7 and 8 are not significantly different. We conclude that regardless of peptide density, large well-spread cells tend to produce stronger traction forces, whereas cells not well spread produce smaller forces.

Discussion

One of the greatest challenges in understanding tissue morphogenesis is deducing mechanisms by which external factors stimulate the reorganization of select cells into three-dimensional structures. For instance, it is still unclear how endothelial cells within a capillary receive signals that cause them to migrate from within a capillary, proliferate, and form new vasculature.¹⁶ The role of ECM in adhesion, migration, and remodeling is a crucial aspect of this challenge. Investigating the role the ECM has in maintaining tractions across a spread cell lends insight into the architecture of cell adhesion and the mechanism of cell migration.

Mechanical stresses within the cell can be exerted externally only if a rigid connection exists.¹ As such, soluble RGD, while amenable to receptor binding, cannot maintain cell shape generated by the tension within the cytoskeleton. To gain insight into the distribution of forces exerted by a cell within our system, a cell adhesion peptide must be chemically linked to a substrate suitable for traction force microscopy. Here, we have presented a technique for immobilizing an RGD-containing peptide on a deformable, otherwise inert, polyacrylamide substrate as a means to study traction forces of spread endothelial cells. The surface-immobilized peptide provides linkage points between a spreading cell and the substrate. As the linkages are formed and the cell imparts a stress onto the substrate through these linkages, the polyacrylamide deforms and, using the technique of traction force microscopy, the deformation within the gel is used to determine the magnitude, direction, and location of these stresses.

Traction Force Studies in BAECs Demonstrate the Balance of Stresses Intrinsic to Cell Adhesion. The distribution of force across the cell provides clues about the architecture of a cell. Several models have been proposed in an attempt to explain cell shape. One can assume that forces acting at sites of integrin attachment to the ECM modify cell function through some form of mechanical connection to the cytoskeleton.²³ Presumably, internal cellular stress is generated and partially loaded onto the "struts" that make up the cytoskeleton. The force generated within the internal contractile apparatus of a cell is balanced by the cell–substrate contacts, as dictated by momentum balance.

Our data imply that the rigid connections that are balancing the internal contractile stress exist primarily under the extensions of the cell rather than directly under the cell body, that is, at the cell periphery. These adhesive interactions between the pseudopodia and substrate would then serve as points that resist compression and support cell shape. Therefore, the force measured in our assay is resultant from the internally generated contractile apparatus of the cytoskeleton and serves to balance the forces that maintain cell shape. A further mapping of cellular structures, such as cytoskeleton and adhesion receptors, is necessary to elucidate the origin of this contractility, and future studies could include inhibiting this contractile apparatus using cytochalasin D or other such inhibitors of the cytoskeleton.

On average, the overall magnitude of the traction force exerted by BAECs is an increasing function of the surface density of RGD peptide. The average cell area has a similar relationship to peptide density such that the ratio of force to area is constant. Despite this average behavior, if one looks at individual cells even at a fixed density of peptide there is considerable variability in both area and force. At all peptide densities, there is a fixed linear relation between the force and the cell area. The average area of a cell in our study is approximately 1350 μm^2 , giving a range, as determined by the concentration of solution in which the gel is incubated, of approximately 200 000 to 2 000 000 molecules of peptide under each cell. These values span a wide range of ligand–integrin interactions on the surface of a typical endothelial cell that can contain on average, a maximum of 1 000 000 $\alpha_v\beta_3$ integrins. Through this range of interactions, the force/area relationship leads to a fundamental constant of 10^4 dyn/cm²,

indicative of a characteristic cell structure that exerts a fixed unit of force. Because both the force and area increase with peptide density, there are three separate hypotheses about the order of mechanistic events. The first is that the increase in peptide concentration causes the increase in force and that the increase in force then triggers the increase in area. The second is that the increase in peptide concentration drives the increase in cell area that then drives the increase in force. And, the third possibility is that the increase in force and area in response to an increase in peptide density are completely independent of each other. Because at even a limited range of peptide densities (Figure 7) the force and area are linearly related, and not independent random variables, the third possibility can be eliminated. Therefore, force and area must be linked.

Our results indicate that a smaller cell exerts a proportionately smaller force than a more spread cell. Therefore, the cellular architecture exerts a fixed level of force on a substrate per unit of area, regardless of the degree of cell spreading. Perhaps, despite forming few focal adhesions, the cell–surface interactions at focal contacts transmit some mechanical signal to the cell that then maintains a constant force-to-area ratio. We speculate that because force and area are still linearly correlated at a fixed RGD concentration, the cell may be like a rubber band that passively resists spreading and the tractions are a driving force that stretches the rubber band. To spread, a cell must produce tractions that stretch the cell membrane and drive actin polymerization. We hypothesize that integrin–ligand binding initiates actin assembly and an increase in traction that results in extension of the plasma membrane, formation of additional receptor–ligand complexes, and an increase in cell area. Therefore, force and area are coupled and increasing force results in an increase in cell area.

Traction Force Distribution in Endothelial Cells Reaffirms the Frontal Towing Model of Migration. Past studies have shown that increasing ligand concentration on a surface has a biphasic relationship to cell migration speed.²² That is to say, at low densities, the cell is unable to establish anchors capable of withstanding the force necessary to move forward, and at too high a density, the adhesions are too strong to be released in order for migration to occur. Maximal migration speed occurs at some intermediate value, where adhesions can both break and form to propel the cell forward and release the rear attachments accordingly. Our results indicate that force increases with spreading, reaffirming the idea that as cell attachments increase, the force that the cell exerts to break attachments and move increases, until attachments are so strong that the cell is unable to exert enough force to break them. Ultimately, using traction force microscopy in time-lapse migration studies will lend insight into the understanding of migration, that is, the optimal force required to attain optimal migration speed.

Acknowledgment. The authors gratefully acknowledge Michael King for assistance with the linear regression and error analysis of Figures 7 and 8. This work was funded by National Institutes of Health Grants HL664388 to D.A.H. and GM61806 to M.D. We are also grateful for support from a Whitaker Foundation Graduate Fellowship to C.A.R.

(21) Li, S.; et al. *Biorheology* **2001**, *38* (2–3), 101–8.

(22) Palecek, S. P.; et al. *Nature* **1997**, *385* (6616), 537–40.

(23) Ingber, D. E. *Annu. Rev. Physiol.* **1997**, *59*, 575–99.